J MATER RES TECHNOL. 2020;9(1):969–983

Available online at www.sciencedirect.com

jmr&t Journal of Materials Research and Technology

www.jmrt.com.br

Original Article

Effect of machinability, microstructure and hardness of deep cryogenic treatment in hard turning of AISI D2 steel with ceramic cutting

Fuat Kara[a,*], *Mustafa Karabatak*[b], *Mustafa Ayyıldız*[a], *Engin Nas*[c]

[a] *Department of Mechanical and Manufacturing Engineering, Technology Faculty, Düzce University, Düzce, Turkey*
[b] *Institute of Science and Technology, Ondokuz Mayıs University, Samsun, Turkey*
[c] *Dr. Engin Pak Cumayeri Vocational School, Düzce University, Düzce, Turkey*

ARTICLE INFO

Article history:
Received 19 September 2019
Accepted 16 November 2019
Available online 4 December 2019

Keywords:
ANN
Machinability
Deep cryogenic
Microstructure
Hardness

ABSTRACT

This study examined the hard turning of AISI D2 cold work tool steel subjected to deep cryogenic processing and tempering and investigated the effects on surface roughness and tool wear. In addition, the effects of the deep cryogenic processes on mechanical properties (macro and micro hardness) and microstructure were investigated. Three groups of test samples were evaluated: conventional heat treatment (CHT), deep cryogenic treatment (DCT-36) and deep cryogenic treatment with tempering (DCTT-36). The samples in the first group were subjected to only CHT to 62 HRc hardness. The second group (DCT-36) underwent processing for 36 h at −145 °C after conventional heat treatment. The latter group (DCTT-36) had been subjected to both conventional heat treatment and deep cryogenic treatment followed by 2 h of tempering at 200 °C. In the experiments, Al_2O_3 + TiC matrix-based untreated mixed alumina ceramic (AB30) and Al_2O_3 + TiC matrix-based TiN-coated ceramic (AB2010) cutting tools were used. The artificial intelligence method known as artificial neural networks (ANNs) was used to estimate the surface roughness based on cutting speed, cutting tool, workpiece, depth of cut and feed rate. For the artificial neural network modeling, the standard back-propagation algorithm was found to be the optimum choice for training the model. Three different cutting speeds (50, 100 and 150 m/min), three different feed rates (0.08, 0.16 and 0.24 mm/rev) and three different cutting depths (0.25, 0.50 and 0.75 mm) were selected. Tool wear experiments were carried out at a cutting speed of 150 m/min, a feed rate of 0.08 mm/rev and a cutting depth of 0.6 mm. As a result of the experiments, the best results for both surface roughness and tool wear were obtained with the DCTT-36 sample. When cutting tools were compared, the best results for surface roughness and tool wear were obtained with the coated ceramic tool (AB2010). The macroscopic and micro hardness values were highest for the DCT-36. From the microstructural point of view, the DCTT-36 sample showed the best results with homogeneous and thinner secondary carbide formations.

* *Corresponding author.*
E-mail: fuatkara@duzce.edu.tr (F. Kara).
https://doi.org/10.1016/j.jmrt.2019.11.037

1. Introduction

In recent years, the cryogenic process has been implemented as a complementary method to the heat treatment of workpieces in order to improve the workability of the materials [1]. The cryogenic process is applied in order to increase wear resistance, generally in materials subjected to high wear. It is a cheap and lasting treatment that is carried out as a single operation and, unlike coatings, is effective on the entire workpiece. The cryogenic process is classified as shallow cryogenic (between −50 °C and −80 °C) and deep cryogenic (temperatures below −125 °C) treatment, depending on the application temperatures on the material. After the heat treatment, the materials are brought to room temperature gradually by keeping them for a predetermined waiting period at shallow or deep cryogenic processing temperatures. With this method, martensite transformation of residual austenite, formation of fine carbide precipitates and homogeneous carbide distribution are achieved in conventionally heat-treated material. Thus, the mechanical properties of materials such as hardness and abrasion resistance are significantly improved [2]. In the vast majority of studies on cryonic processing retention time, the ideal waiting time was found to be 36 h [3–6].

Das [7] aimed to determine the optimum holding time by investigating the effects of deep cryogenic processing applied at −196 °C for different retention times of 0–132 h on the wear properties, hardness values and microstructural characteristics of AISI D2 cold work tool steel. As a result of the study, deep cryogenic processing was shown to increase wear resistance. As demonstrated by microstructure photographs and hardness and surface roughness values, the highest wear resistance increase (84.88%) was obtained in cryogenic samples held for 36 h. In a study conducted by Amini et al., the AISI D3 cold work tool steel was subjected to different curing times (24, 36, 48, 72, 96 and 120 h) at deep cryogenic processing temperatures to determine the microstructural, carbide distribution and macro and micro hardness variations depending on cryogenic processing holding time. Microstructural changes in the AISI D3 tool steel specimen deep cryogenically treated for 36 h showed the best result in terms of carbide distribution and macro and micro hardness [8]. In his study, Kara [6] investigated the effect of deep cryogenic processing (−145 °C) on the microstructure and mechanical properties of AISI 52100 bearing steel at different retention times (12, 24, 36, 48 and 60 h). Among the deep cryogenically treated samples, the best mechanical properties were obtained at 36 h of deep cryogenic treatment. Moreover, the 36-h deep cryogenically treated specimens also showed the best microstructural properties with more homogeneous microstructure and thinner carbide precipitation. Taking into account the results of the research carried out in the literature, the duration of deep cryogenic treatment was chosen as 36 hours in this study.

Nowadays, a whole range of neural network methodologies have been developed that model the correlation between the input and the output parameters of the turning process [6]. Ozel and Karpat [9] used regression and artificial neural network (ANN) models for estimating the surface roughness and tool wear in the hard turning of AISI H13 steel using CBN inserts. Davim and Figueira [10] studied the influence of cutting speed and feed rate on flank wear, specific cutting force and surface roughness in the hard turning of AISI D2 cold work tool steel using conventional ceramic inserts and statistical techniques. Ozel and Karpat [11] investigated the machining of AISI D2 steel using multi-radii/wiper mixed alumina ceramic inserts with TiN coating and developed an ANN for predicting tool wear and surface roughness. Quiza [12] compared statistical models with an ANN for estimating tool wear in the hard turning of AISI D2 steel using conventional ceramic inserts. Kumar [13] focused on the investigation of flank wear, average surface roughness and chip-tool interface temperature in the machine turning of heat-treated AISI D2-grade tool steel using coated carbide inserts. Response surface methodology (RSM) based models and ANN models were implemented to estimate the responses in hard-turning.

Although AISI D2 cold work tool steel has a very widespread application area, studies carried out on the workability of this material were found to be very limited in the literature, and indeed, no study has to date examined the machinability of AISI D2 cold work tool steel subjected to cryogenic treatment, although there are studies that examine the effects of cryogenic processing on machinability for different types of materials. This situation necessitated a study to be carried out. This study aimed to improve cutting conditions by applying in addition to heat treatment, deep cryogenic treatment and deep cryogenic treatment + tempering and to investigate the materiasl under processing conditions using coated and uncoated ceramic tools. By improving the cutting conditions, the aim was to decrease the surface roughness and reduce machining costs by increasing tool life.

This study consists of three parts. The first part evaluates AISI D2 cold work tool steel with three different heat treatments (conventional heat treatment, conventional heat treatment + deep cryogenic processing and conventional heat treatment + deep cryogenic processing + tempering), using different cutting tools and different cutting speed, feed rate and depth of cut combinations. The surface roughness of the machined deep cryogenically treated cold work tool steel workpiece and the effects on tool wear are discussed. The second part investigates the effects of conventional heat treatment, conventional heat treatment + deep cryogenic processing and conventional heat treatment + deep cryogenic procesing + tempering on the microstructure and macro and micro hardness of AISI D2 cold work tool steel material. The third part estimates the experimental values of surface roughness (Ra) using ANN.

2. Material and methods

2.1. *Workpiece, machine tools and cutting parameters*

Cylindrical AISI D2 cold work tool steel in dimensions of Ø60 × 300 mm was used. The chemical composition of the test samples is given in Table 1. The hard turning experiments were performed on a GOODWAY GLS-1500 CNC lathe using an uncoated SNGA 120408 T01020 AB30 turning tool and SNGA1204 08 T01020 AB2010 ceramic turning tips manufactured by TaeguTec cutting tool company to perform the hard

Table 1 – Chemical composition (%) of test samples.

C	Si	Mn	P	S	Cr	Mo	V
1.575	0.32	0.30	0.024	0.0020	11.70	0.74	0.960

lathe tests. A PSBNR 2525 M12 turning tool holder was used to connect the cutting tools.

Hard turning experiments were carried out at three different cutting speeds (50, 100, 150 m/min), three different feed rates (0.08, 0.16 and 0.24 mm/rev) and three different cutting depths (0.25, 0.50 and 0.75 mm). Two different types of ceramic tools (with and without coating) were tested under dry cutting conditions on material subjected to conventional heat treatment, conventional heat treatment + deep cryogenic processing and traditional heat treatment +36 h deep cryogenic processing + tempering. A total of 162 cutting tests were carried out in each combination. For each cutting tool, the tool wear tests were performed according to different machining times at a constant cutting speed, feed rate and cutting depth. Table 2 gives the parameters used in the surface roughness and tool wear tests.

2.2. *Deep cryogenic treatment*

The test specimens were divided into three batches, CHT (Traditional Heat Treatment), DCT-36 (Traditional Heat Treatment +36 h Deep Cryogenic Processing) and DCTT-36 (Traditional Heat Treatment +36 h Deep Cryogenic Processing + Tempering). The AISI D2 cold work tool steel had been subjected to preheating, austenitizing and tempering prior to cryogenic processing. The preheating process involved 30 min at 450 °C, 60 min at 650 °C and 30 min at 850 °C. After preheating, the samples were austenitized by heating in an atmosphere-controlled furnace at 1030 °C for 60 min. After the austenitizing process, rapid cooling in nitrogen was performed at 4 bar pressure in a vacuum oven. Finally, the samples were tempered at 200 °C for 180 min and at 350 °C for 180 min to a hardness of 60–62 HRc. Deep cryogenic treatment was then applied to the DCT-36 and DCTT-36 samples at −145 °C for 36 h. Finally, for the DCTT-36 sample, the heat treatment and cryogenic processing was completed by tempering at 200 °C for 180 min. Table 3 shows the conventional heat treatment and deep cryogenic processes applied to the AISI D2 cold work tool steel.

Table 3 – Heat treatment and deep cryogenic processing.

AISI D2 cold work tool steel		
Process	Temperature	Time
1. Preheating	450 °C	30 min
2. Preheating	650 °C	60 min
3. Preheating	850 °C	30 min
austenitizing	1030 °C	60 min
Cooling	4 Bar Nitrogen cooling at pressure	–
1. Tempering	200 °C	180 min
2. Tempering	350 °C	180 min
Deep cryogenic process	−145 °C	36 hour
Tempering	200 °C	180 min

2.3. *Measurement of surface roughness and tool wear*

Measurement and evaluation of surface roughness is very important in workability studies [14]. The Taylor Hobson Surtronic 25 surface roughness tester was used to measure the surface roughness of the machined surfaces. The surface roughness was measured in three places from the treated surfaces and their average determined the roughness (Ra) values. The effects of the AISI D2 cold work tool steel subjected to different heat treatments on the wear performance of the coated and uncoated ceramic cutting tools under hard turning conditions were investigated at a constant cutting speed, feed rate and cutting depth. The CHT, DCT-36 and DCTT-36 specimens were machined with uncoated and coated ceramic tools at a cutting speed of 150 m/min, a feed rate of 0.08 mm/rev and a cutting depths of 0.6 mm and were subjected to hard turning (2, 4 and 6 min) and tool wear tests were carried out. During the abrasion tests, the cutting process was stopped at certain intervals and the worn surfaces were photographed by the Dino-Lite digital microscope. After the width of the cutting tool (4.76 mm) was introduced in the Dino Capture 2.0 program, the amount of nose and crater wear on the tool was measured. The amount of cutting tool wear was evaluated depending on the heat treatment type and machining time. In addition, by

Table 2 – Surface roughness and tool wear test parameters.

Surface roughness tests				
Cutting tool	AB30		AB2010	
Heat treatment	CHT	DCT-36		DCTT-36
Cutting speed (V, m/min)	50	100		150
Feed rate (f, mm/dev)	0.08	0.16		0.24
Cutting depth (a, mm)	0.25	0.50		0.75
[10pt] Tool wear tests				
Cutting tool	AB30		AB2010	
Heat treatment	CHT	DCT-36		DCTT-36
Cutting speed (V, m/min)	150			
Feed rate (f, mm/dev)	0.08			
Cutting depth (a, mm)	0.6			
Processing time (Ct, min)	2	4	6	8	10

photographing the abraded surfaces with the SEM device, the types of abrasion formed were determined. In order to determine crater wear, SEM photographs were taken on a 1:1 scale in a CAD environment, the crater zones were precisely drawn and their areas were calculated.

2.4. SEM and hardness analyses

Hardness measurements of the test specimens were made on both micro and macro hardness testers. For both hardness measurements, a total of 36 specimens were prepared, 12 of which were 10 × 10 mm. Each macro and micro hardness measurement reflected the average of at least 10 hardness measurements. Micro hardness measurements were performed with a Metkon microhardness tester. Macro hardness measurements were made using the Rockwell (HRc) hardness measurement method with the Bulut Makina macrohardness tester. One 10 × 8 mm sample was prepared for each type of heat treatment for use in the microstructure studies. After conventional heat treatment, 36 h of deep cryogenic treatment and 36 h of deep cryogenic treatment + tempering, sanding with 120, 240, 600, 800 and 1200 grit SiC sand paper was carried out on the samples and they were then polished in the sample shaver for about 5 min. They were then examined by optical microscopy and prepared for scanning electron microscopy (SEM) imaging with 3% Piccale (97 mL of ethyl alcohol, 3 g of picric acid). In terms of resolution, SEM is at 2000 Å and optical microscopes at 25 Å, while the scanning depth in scanning electron microscopy is 300–600, which is 30× higher than in optical microscopy. For this reason, the microstructure photographs were taken with an FEI Quanta FEG 250 scanning electron microscope for more detailed high magnification.

2.5. Artificial neural networks

Artificial neural networks (ANNs) imitate some basic aspects of the brain functions [15,16]. A neuron is the basic element of the neural networks, and its shape and size may vary depending on its functions [17]. The simplest neural network is composed of neurons, inputs, weights and a summation function, activation function and output. The summation function calculates the net input of the neuron, as shown in Eq. (1).

$$NET_i = \sum_{j=1}^{n} w_{ij}x_j + w_{bi} \quad (1)$$

Where NET_i is the weighted sum of the input to the ith processing element, n the number of processing elements in the previous layer, i and j the processing elements, w_{ij} the weights of the connections between ith and jth processing elements, x_j the output of the jth processing element and w_{bi} the weights of the biases between layers. The activation function, which processes the net input of the neuron, defines the output of the neuron. Many functions such as the threshold function, step activation function, sigmoid function, and hyperbolic tangent function are used to define the activation function. The sigmoid function is generally used for the transfer function and generates a value between 0 and 1 for each value of the net input. The logistic transfer function of the ANN model improved in this study is given in Eq. (2).

$$f(NET_i) = \frac{1}{1 + e^{-NET_i}} \quad (2)$$

The optimal learning algorithm and network structure should be determined to obtain the output values closest to the experimental values. To this end, the number of neurons in the hidden layer was boosted step by step (i.e., from ten to fifteen), and quasi-Newton back propagation (BFGS), conjugate gradient back propagation (CGP), Levenberg–Marquardt (LM), resilient back propagation (RP), and scaled conjugate gradient (SCG) learning algorithms were used to define the optimal network structure and learning algorithm. The trials conducted in this study showed the LM learning algorithm to be the best learning algorithm for the surface roughness. The determination of the best learning algorithm and optimal number of neurons for the surface roughness are given in Table 4.

Table 4. Statistical data of surface roughness for five learning algorithms.

Table 4 – Statistical data of surface roughness for five learning algorithms.

Learning algorithm	Number of neurons	Training data		Testing data	
		RMSE	R^2	RMSE	R^2
BFGS	5-10-1	0.0963	0.9523	0.0930	0.9540
BFGS	5-11-1	0.1005	0.9528	0.0913	0.9591
BFGS	5-12-1	0.1091	0.9387	0.1083	0.9337
BFGS	5-13-1	0.1042	0.9587	0.0952	0.9638
BFGS	5-14-1	0.1149	0.9428	0.1076	0.9480
BFGS	5-15-1	0.1336	0.9426	0.1250	0.9465
CGP	5-10-1	0.0991	0.9425	0.0954	0.9448
CGP	5-11-1	0.0929	0.9500	0.0896	0.9512
CGP	5-12-1	0.0830	0.9649	0.0770	0.9680
CGP	5-13-1	0.0974	0.9515	0.0938	0.9533
CGP	5-14-1	0.1163	0.9485	0.1017	0.9572
CGP	5-15-1	0.1021	0.9595	0.0950	0.9628
LM	5-10-1	0.0906	0.9572	0.0821	0.9630
LM	5-11-1	0.0766	0.9741	0.0720	0.9763
LM	5-12-1	0.1005	0.9478	0.0900	0.9568
LM	5-13-1	0.1055	0.9414	0.0981	0.9476
LM	**5-14-1**	**0.0783**	**0.9704**	**0.0692**	**0.9755**
LM	5-15-1	0.0841	0.9655	0.0798	0.9666
RP	5-10-1	0.0956	0.9642	0.0921	0.9656
RP	5-11-1	0.1021	0.9613	0.0952	0.9649
RP	5-12-1	0.1030	0.9410	0.1080	0.9312
RP	5-13-1	0.0775	0.9714	0.0721	0.9738
RP	5-14-1	0.0793	0.9736	0.0709	0.9778
RP	5-15-1	0.1092	0.9329	0.1044	0.9367
SCG	5-10-1	0.0946	0.9473	0.0931	0.9453
SCG	5-11-1	0.0859	0.9573	0.0905	0.9498
SCG	5-12-1	0.1020	0.9386	0.0956	0.9426
SCG	5-13-1	0.0839	0.9650	0.0754	0.9705
SCG	5-14-1	0.0914	0.9650	0.0750	0.9755
SCG	5-15-1	0.0890	0.9588	0.0828	0.9623

There were five input parameters in the network: cutting tool (ct), workpiece (wp), cutting speed (V), depth of cut (dp), and feed rate (f). There was one output parameter in the network as the surface roughness (Ra). The best network structure was identified as 5-14-1 (Fig. 1). As a result of the tests, the experimental data obtained (162 for each input and output)

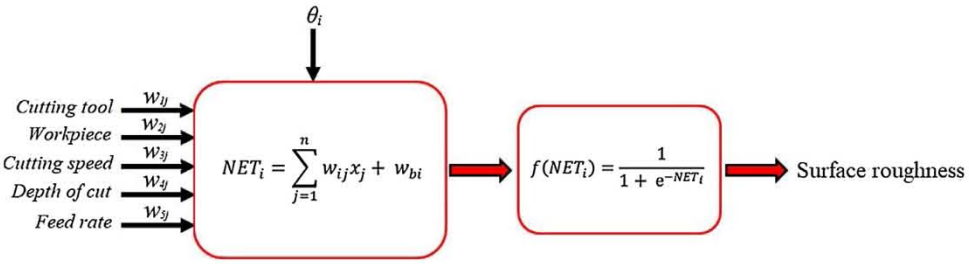

Fig. 1 – Optimal network structure.

were prepared for the testing and training sets of the ANN. The ratio for testing and training data was selected as approximately 15:85, i.e., 32 and 130 sets of all experimental data were arbitrarily selected for the testing and training data, respectively. In this study, the input and output values were normalized between 0 and 1 to attain better predictions. The surface roughness values estimated after ANN training were checked against the experimental data.

The root mean square error (RMSE) and correlation coefficient (R^2) values were used for comparison. The most precise technique for the problem under study was chosen from the algorithms of the state-of-the-art for regression. The RMSE was used to compare the regressors. This metric measures the deviation that the predicted class value has with regard to its real value [17]. Eqs. (3) and (4) give the formulae for the RMSE and R^2 [18,19].

$$\mathrm{RMSE} = \left(\left(\frac{1}{p}\right) \sum_j \left| t_j - o_j \right|^2 \right)^{1/2} \tag{3}$$

$$R^2 = 1 - \left(\frac{\sum_j \left(t_j - o_j\right)^2}{\sum_j \left(o_j^2\right)} \right) \tag{4}$$

where, t is the goal value, o is the output value, and p is the number of samples.

3. Experimental results

3.1. *Outputs of surface roughness*

The AISI D2 cold-work tool steel was subjected to conventional heat treatment (CHT), 36-h deep cryogenic treatment (DCT-36) and 36-h deep cryogenic treatment + tempering (DCTT-36). The cutting parameters and the changes that occurred in surface roughness depending on cutting conditions after the hard turning tests using coated and uncoated ceramic tools are shown in Fig. 2. In general, surface roughness (Ra) values were found to vary between 0.22 μm and 3.1467 μm. The Ra values tended to decrease for both tools with increasing cutting speed for all of the cutting parameter values. The increase in cutting speed reduced the tool-to-chip contact area, thereby reducing friction, which allowed for better surface quality to be achieved. Some researchers, however, have argued that the decrease in Ra due to increased cutting speed is due to the reduced tendency toward stacking chip formation [20–22]. However, at high cutting speed (150 m/min), the tool wear values were slightly increased. In this case, the increased tool wear can be explained by the increase of the load on the cutting tool and the high temperatures generated while cutting at high speed.

After a 300% increase in cutting speed, the surface roughness values improved by 52% at low feed rate (0.08 mm/rev) values. However, when high feed rate (0.24 mm/rev) values were reached, Ra values decreased by 45% up to a cutting speed of 100 m/min. Although when a 50% increase in cutting speed to 150 m/min was reached, Ra increases of up to 25% were seen. This can be explained by the decrease in tool chip contact area with the increase of cutting speed, the tool wear with the high cutting parameters and the excessive deformation of the machined surface [23].

Feed rate is one of the important parameters that determines the character of the cutting process [24,25]. In terms of cutting parameters and cutting tools, increasing feed rates have been found to be an important factor in increasing surface roughness values. Kacal [26] studied the effect of variation in feed rate values on the surface roughness of PMD-23 steel produced by the T / M method and evaluated tool wear and surface roughness in turning using coated ceramic cutting tools. As the feed rate increased, the Ra values measured for all tools were also seen to increase. The Ra values at the lowest feed rate (0.08 mm/rev) for all of the machining parameters ranged between 0.18 and 1.723 μm while the Ra showed a significant increase at the highest feed rate (0.24 mm/rev), reaching a value of 3.41 μm. Increasing the feed rate caused the shear forces and vibration to increase by increasing the chip volume removed at the unit time, thus increasing the surface roughness. In addition, increase in the feed rate as well as the cutting speed caused the temperature at the cutting tool-workpiece interface to increase. The temperature increase at the interface then led to tool wear and consequently caused the surface roughness to deteriorate. This indicated that there was a direct relationship between tool wear and surface roughness, as stated in the literature studies [27,28].

Looking at Fig. 2, it can be seen that Ra increased with increasing depth of cut. The Ra values are in the range of 0.18–3.14 μm at 0.25 mm cutting depth, 0.23–3.08 μm at 0.50 mm cutting depth and 0.23–3.41 μm at 0.75 mm cutting depth. The best surface roughness value was 0.18 μm at 0.25 mm cutting depth and the highest Ra value was 0.75 mm at a cutting depth of 3.41 μm. Increased depth of cut and increased surface roughness have been confirmed by numerous literature studies [29]. The depth of cut also directly affects

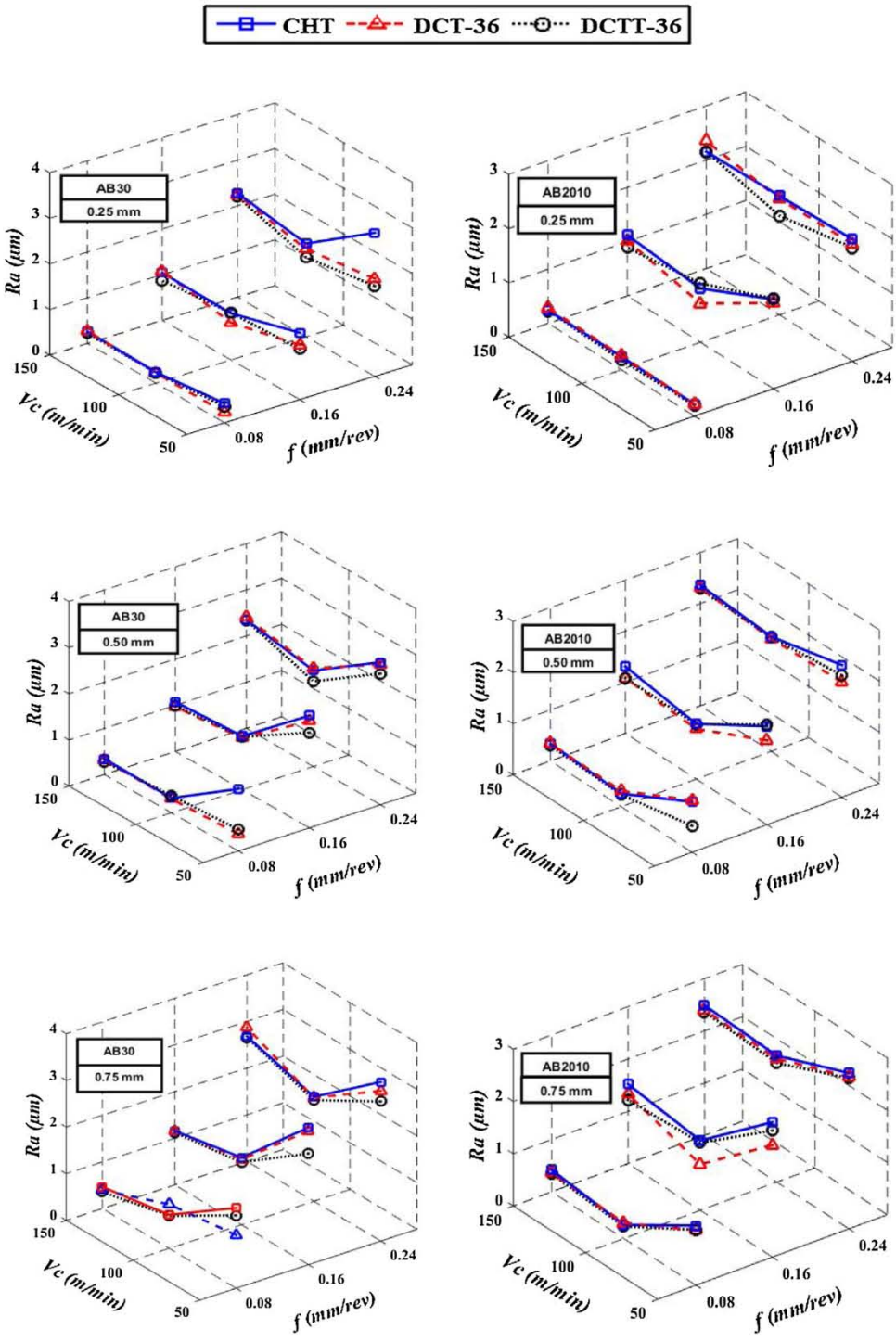

Fig. 2 – Surface roughness (Ra) values.

the cross section area of the kerf that the cutting tool tried to remove during the cutting process. The first important factor in terms of the effect of depth of cut on the surface roughness is the chip formation. It is known that Ra is decreased as the chip size decreases [23]. Along with increased chip size, the slip plane area in the first deformation zone also grows and makes the cutting process difficult. Therefore, the cutting force values and thus the surface roughness are increased.

The second factor is the cutting temperature. There are different mechanisms that influence the temperature during cutting. Plastic deformation primarily occurs in the first deformation zone. Heat energy is generated by friction and plastic deformation in the second deformation zone and finally, heat energy is formed in the region called the third deformation zone, where the flank surface of the cutting tool comes into contact with the workpiece [30,31]. In particular, the increases in the feed rate and cutting depth increase the area of the slip

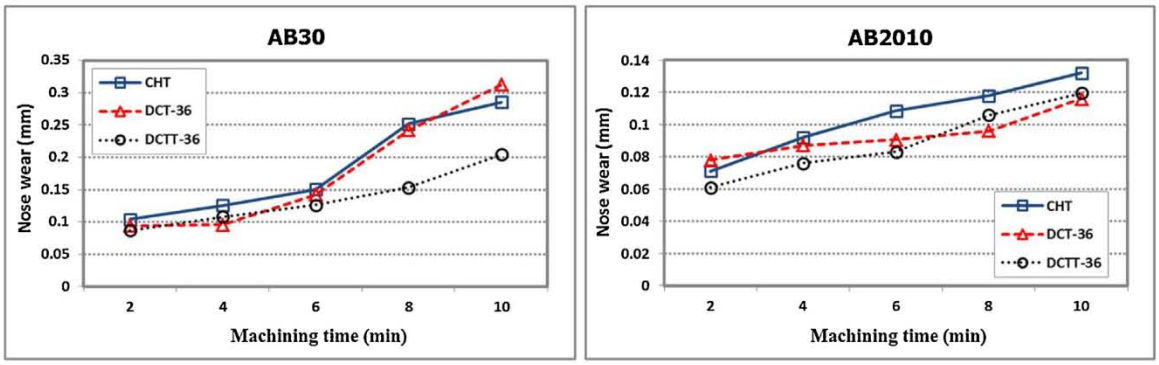

Fig. 3 – Change in nose wear according to machining time and heat treatment type.

surface in the first deformation zone, so that more energy is required to break off chip from the surface and more heat is released as a result of this consumed energy. In addition, with the increase in chip size, the friction in the tool-chip interface increases in the second deformation zone, thus affecting the cutting temperature. Cutting tool wear occurs parallel to the increase of the cutting temperature. The quickly worn cutting tool causes worse surface roughness. In addition, increase in depth of cut causes an increase in surface roughness.

3.2. *Outputs of nose and crater wear*

3.2.1. *Change of nose wear according to heat treatment type*

A series of wear tests were conducted under dry cutting conditions to investigate the effect of tempering after conventional heat treatment on tool life, deep cryogenic treatment and deep cryogenic treatment with tempering applied to the AISI D2 cold work tool steel. Tool wear experiments were carried out using two tool types, Al_2O_3+TiC matrix-based uncoated mixed alumina ceramic tools (AB30) and Al_2O_3+TiC matrix-based TiN PVD-coated ceramic tools (AB2010), at a cutting speed of 150 m/min, a feed rate of 0.08 mm/rev and depth of cut of 0.6 mm for five different processing times (2, 4, 6, 8 and 10 min). As a result of abrasion tests, both nose and crater wear generally occurred on both tools. At the end of the machining times, the nose wear values were measured linearly on a precision camcorder.

Nose wear changes are given in Fig. 3. From the wear values obtained for both cutting tools, an average increase of 138% in nose wear values can be seen for the CHT specimen when machining time was increased five-fold from 2 to 10 min. For the DCT-36 and DCTT-36 samples, this ratio was found to be 149% and 119%, respectively. According to heat treatment type, the lowest nose wear values, like those for surface roughness, were also obtained with the DCTT-36 sample. When all processing times were taken into account according to heat treatment type, the lowest nose wear values were obtained with the DCTT-36 sample.

With the increase in machining time, the heat generated in the cutting zone also rose in parallel. This increase in the amount of heat caused the temperature at the cutting tool-workpiece interface to rise. Cutting tools maintain their properties up to a certain temperature value. When the cutting tool limit values are reached, they will be subjected to plastic deformation. After permanent deformation, various types of wear occur in the cutting tool and it loses its function. For this reason, the amount of wear increases in parallel with the increase in processing time [32]. It is stated in the literature that dependent on increasing machining time, the wear on the cutting tool and hence the surface quality is worsened [33]. Lima [34] used three different cutting tools to perform hard turning on AISI 4340 and AISI D2 cold work tool steel to investigate cutting tool life and surface roughness according to machining time. It was found that during the 0–20 min time period the machining had worn out the residual cutting tool life.

3.2.2. *Change of nose wear according to cutting tool*

The machining time, type of cutting tool and nose wear changes according to the heat treatment type are shown in Fig. 4. The nose wear values varied between 0.061 mm and 0.312 mm. When the average nose wear values obtained for the CHT, DCT-36 and DCTT-36 samples were taken, it was seen that the wear time for the AB30 uncoated ceramic tool had increased by 181% with the five-fold increase of processing time from 2 to 10 min. A 75% increase in nose wear was seen in the AB2010 coated ceramic cutting tool with the five-fold increase from 2 to10 min of processing. At the end of the 10-min treatment period, the lowest nose wear value of 0.061 mm was obtained with the AB2010 cutting tool on the DCTT-36 specimen. When comparing the coated and uncoated cutting tools and considering all machining times, the lowest nose wear values were obtained with the AB2010 coated ceramic tool (Fig. 4).

The nose wear values were in parallel with those of studies in the literature [27,35–37]. Dosbeva [38] conducted a study on the hard turning of AISI D2 cold work tool steel in order to compare wear on CVD-coated tungsten carbide and PCBN cutting tools according to machining time. Nose wear was seen in both tools, while the lowest nose wear value was obtained with the PCBN tool.

3.2.3. *Change of crater wear according to heat treatment type*

The crater wear values at 150 m/min cutting speed, 0.08 mm/rev feed rate and cutting depth of 0.6 mm at different machining times were determined by calculating

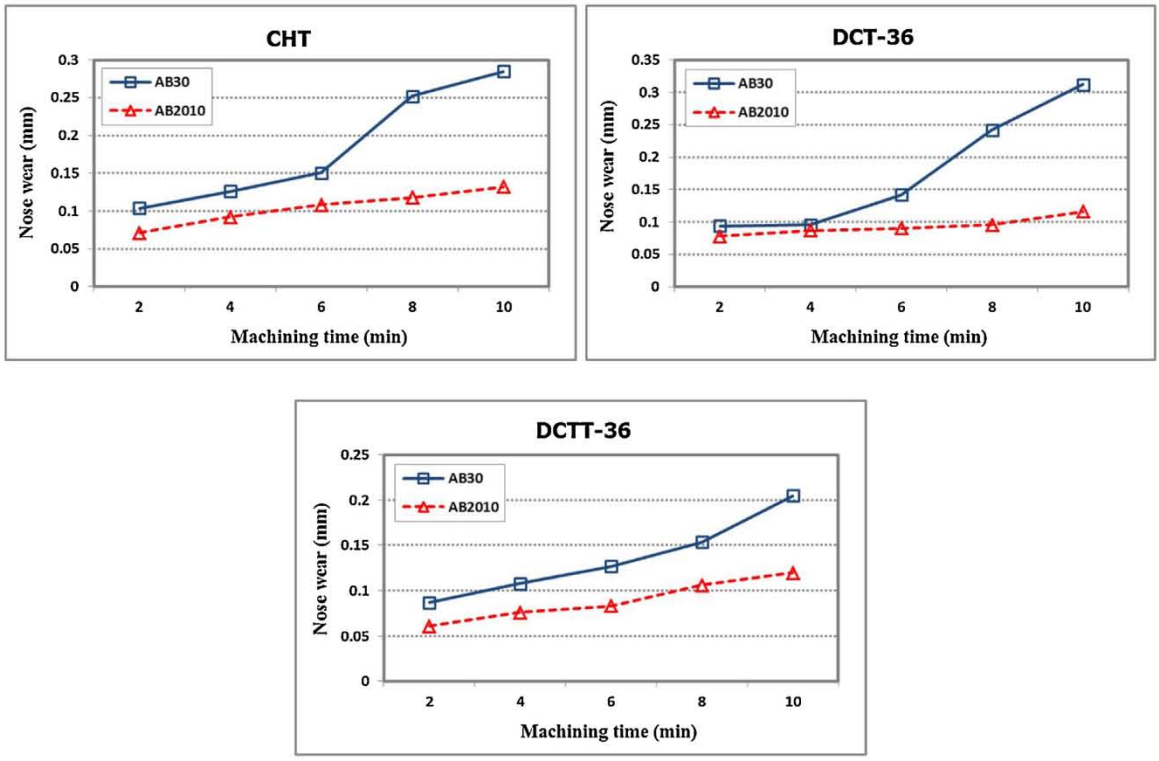

Fig. 4 – Changes in nose wear according to machining time and cutting tool type.

the surface area of the craters in a CIS (Computer Aided Design) environment. Crater wear changes are given in Fig. 5. When the wear values obtained with both cutting tools were taken, the Fig. 5 shows an average increase of 267% in nose wear values for the CHT sample with a five-fold increase from 2 to10 min of processing time. For DCT-36 and DCTT-36 samples, this ratio was found to be 173% and 158%, respectively. When all processing times were taken into account, the lowest crater wear values were obtained with DCTT-36 as compared to the other heat treatment types. The DCT-36 sample then provided the lowest crater wear, while the highest wear values were seen with the conventionally heat-treated CHT sample. This was attributed to the improvement of the mechanical properties of the cutting tool material and the more homogeneous microstructure resulting from the cryogenic processing and subsequent tempering [39,40]. Thanks to the cryogenic processing, there was a positive increase in the wear resistance of the cutting tool material and likewise, a more evident homogeneous arrangement in the microstructure. After these two positive situations, it was supposed that the tool wear on the abraded surfaces of the cutting tool during cutting would occur at a lower rate.

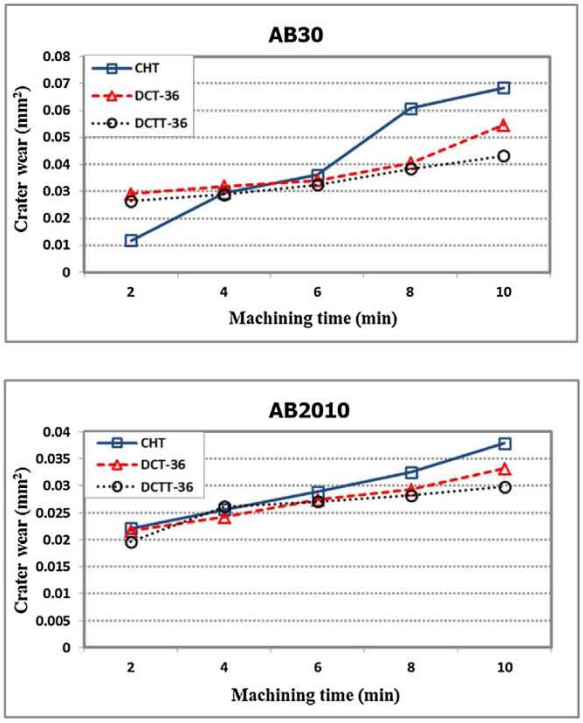

Fig. 5 – Change in crater wear according to machining time and heat treatment type.

3.2.4. *Change of crater wear according to cutting tool*

The machining time, type of cutting tool and changes in crater wear dependent on heat treatment type are shown in Fig. 6. It can be seen that crater wear values changed between 0.0177 mm^2 and 0.0684 mm^2. When the average crater wear values obtained for the CHT, DCT-36 and DCTT-36 samples were taken, there was a 227% increase in crater wear in the AB30 uncoated ceramic tool with the five-fold increase from 2 to 10 min machining time. In the AB2010 coated ceramic cutting tool, there was a 159% increase in the crater wear with the 5-fold increase in machining time from 2 to10 min. At the end

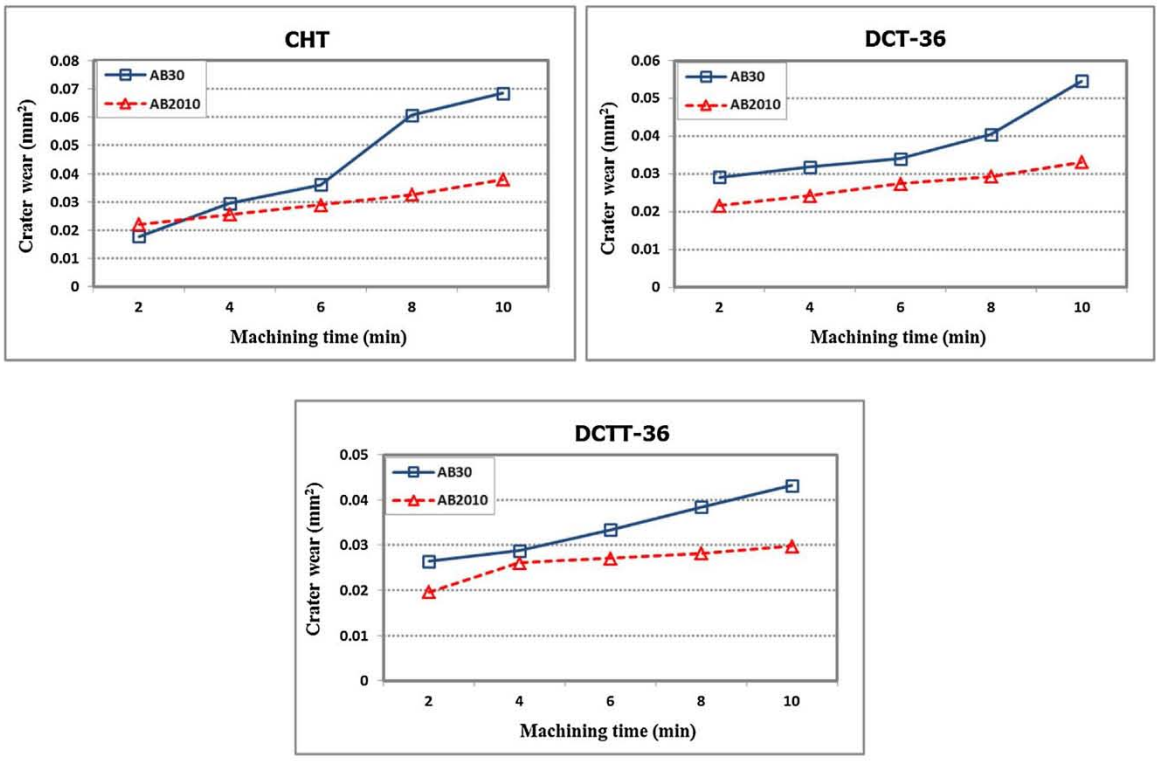

Fig. 6 – Change of crater wear according to machining time and cutting tool type.

of the 10 min machining cycle, the lowest crater wear value of 0.0298 mm^2 was obtained with the AB2010 cutting tool on the DCTT-36 specimen. The lowest wear values for CHT and DCT-36 specimens were 0.0379 mm^2 and 0.0332 mm^2, respectively. When all machining times were considered and the coated and uncoated cutting tools were compared, the lowest crater wear was obtained with the AB2010 coated ceramic tool. Compared to the TiN-coated ceramic tool (AB2010) Al_2O_3 + TiC matrix-based uncoated composite alumina ceramic tool (AB30), the Al_2O_3 + TiC matrix-based PVD-coated tool resulted in 164.% lower crater wear after 10 min machining time. This result was associated with a low coefficient of friction and good crater wear resistance, although the TiN coating on the top layer of this cutting tool is not a very hard material [25,33].

It is possible to say that the crater wear values increased with the increase in the machining time. The change of crater wear over time is like the change of nose wear over time. Moderate crater wear does not usually limit tool life. Indeed, the formation of craters enhances the effectiveness of the tool thread angle and thus reduces the cutting forces. However, excessive crater wear will weaken the cutting edge and this will cause deformation or fracture of the tool [33,41]. This results in worsening quality of the workpiece surface and causes wear types such as flank wear and crater wear on the surface of the cutting tool and edge regions.

3.3. *Outputs of microstructure and hardness*

3.3.1. *Outputs of microstructure*

Microstructure views of the test specimens are given in Fig. 7. The CHT sample exhibited a non-uniform carbide distribution, while the DCT-36 sample exhibited a uniform primary carbide and a nearly spherical secondary carbide distribution. However, after the 36-h deep cryogenic processing + tempering (DCTT-36), the carbide dimensions decreased and a more homogeneous carbide distribution was observed. When the heat treated specimens are compared with each other, it can be seen that the microstructure of the DCTT-36 sample is thinner and has a more homogeneous structure. Das [7,42] investigated changes in microstructure by performing deep cryogenic processing and subsequent tempering at different holding times (0, 12, 36, 60 and 84 h) on the AISI D2 cold work tool. As a result of the study, they reported that the highest percentage of carbide was in the deep cryogenic sample for 36 h. If a general assessment of the microstructure studies is made, the deep cryogenic processing + tempering appears to have provided more homogeneous and more dense carbon distribution. In addition, it was determined that the results obtained from the microstructure studies are in concurrence with the studies in the literature.

3.3.2. *Outputs of hardness*

3.3.2.1. Change of macro hardness. Fig. 8 shows the change in micro hardness values of AISI D2 cold work tool steel subjected to different heat treatment and deep cryogenic processes. As can be seen in Fig. 8, the highest hardness values are respectively in the DCT-36, DCTT-36 and CHT specimens. The hardnesses of CHT, DCT-36 and DCTT-36 were measured as 62.2, 63.1 and 62.8 HRc, respectively. Macroscopic recoveries of deep cryogenically treated samples according to conventionally heat treated samples were found to be 1.44% and 0.96% for DCT-36 and DCTT-36, respectively. The highest macro-

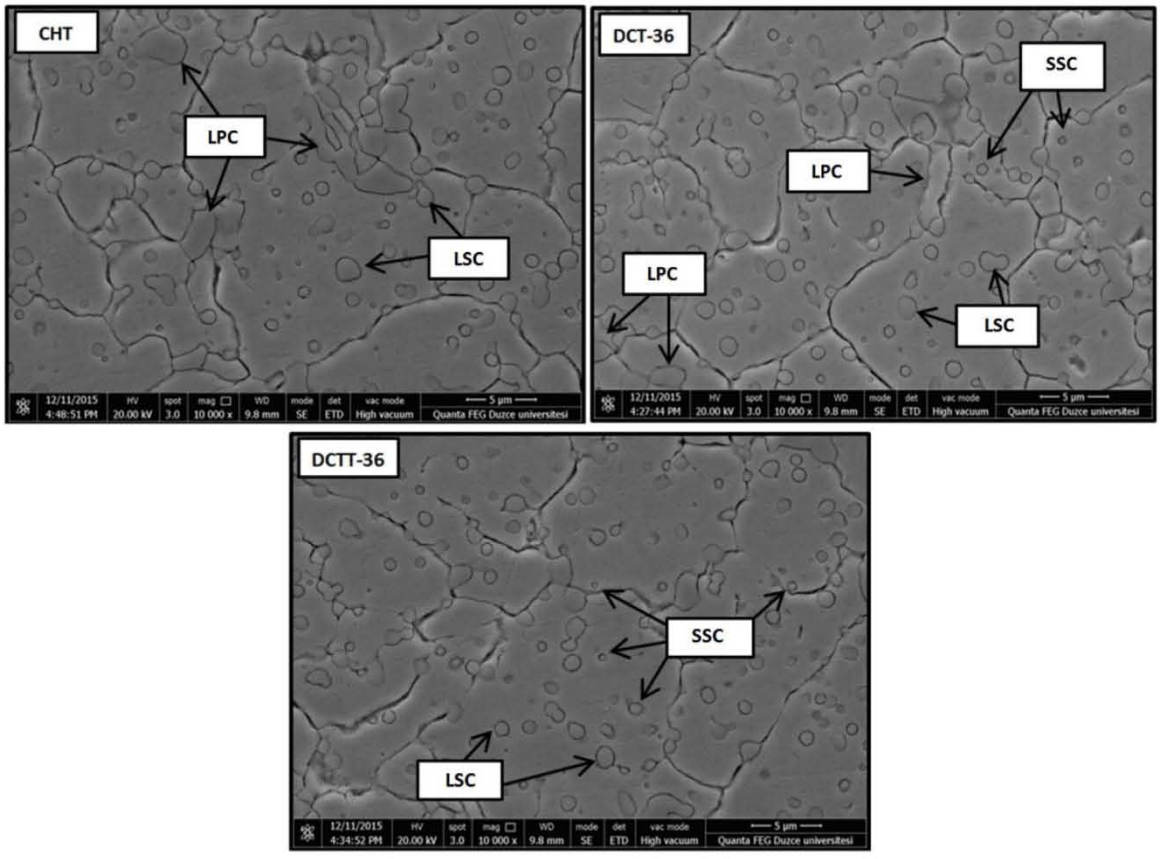

Fig. 7 – Microstructure views of AISI D2 cold work tool steel samples (LPC - Large primary carbides, LSC - Large secondary carbides, SSC - Small secondary carbides).

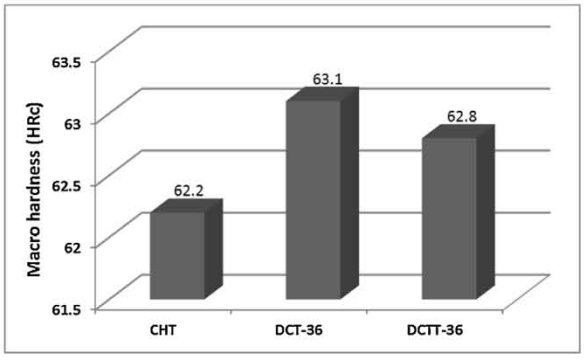

Fig. 8 – Change of macro hardness values according to heat treatment type.

scopic value among the heat-treated samples was obtained at the DCT-36 sample. This was attributed to the fact that the austenite martensite transformation in the microstructure of the material with the cryogenic processing occurred at a higher rate in the DCT-36 sample than in the CHT and DCTT-36 samples [6,43–46]. The AISI D2 cold work tool steel has a soft inner structure, which transforms from the austenite phase into a harder martensite phase, resulting in a stiffer structure. Tempering after deep cryogenic processing caused a slight decrease in hardness. For this reason, the hardness of the DCTT-36 sample measured at higher values than the CHT sample, but was lower than the DCT-36 sample.

Similar results have been observed in the literature [46]. In their study, found a 22% increase in the macroscopic extent of carbide material with deep cryogenic processing [45]. In another study, Rhyim et al. (2006) suggested that deep cryogenic processing improves stiffness. Sonawane [47] performed conventional heat treatment, deep cryogenic processing and deep cryogenic processing plus tempering on M2 tool steel. They noted that the highest macro hardness value was obtained from the deep cryogenic sample.

3.3.2.2. *Change of micro hardness.* Fig. 9 shows the micro hardness variations of AISI D2 cold work tool steel samples. The graph shows that the highest micro hardness values were obtained with the DCT-36, DCTT-36 and CHT samples as 871.8 HV, 748.46 HV and 618.46 HV, respectively. The change in micro hardness values was in parallel with the macro hardness results. Improvements in micro hardness values were found to be 41% and 21% for DCT-36 and DCTT-36, respectively. When the heat treatments applied to the material were compared, the highest micro hardness value was obtained with the DCT-36 sample. This was attributed to the fact that with the deep cryogenic processing, the austenite-martensite transformation in the microstructure of this sample took place at a higher rate than in the other samples, resulting in a more brittle structure.

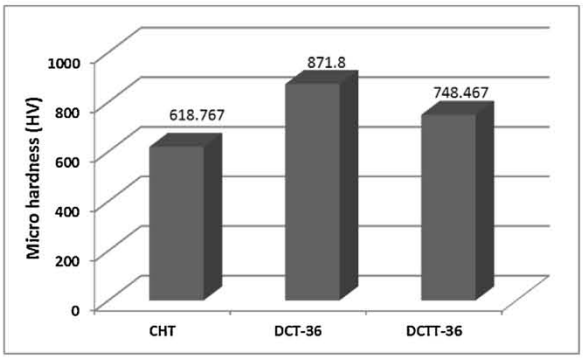

Fig. 9 – Changes of micro hardness values according to heat treatment type.

The micro hardness results were in agreement with the literature [48–51]. Das [52] in their work, showed that among the AISI D2 cold work tool steel samples subjected to conventional heat treatment, shallow cryogenic processing, and deep cryogenic processing, the deep cryogenic sample reached the highest micro hardness values [48]. Oppenkowski [53] reported that after 24–36 h of cryogenic treatment, the micro hardness of AISI D2 cold work tool steel was higher in the 36-h cryogenically treated samples. Amini [54] reported that deep cryogenic processing at different retention times increased stiffness and achieved the highest hardness values in terms of both macro and micro hardness for the tool life. Nanesa [48] applied different heat treatments to AISI D2 cold work tool steel. Improvements in microhardness values were found to be 7.7% for deep cryogenically treated samples compared to conventionally heat-treated samples. In their study, Amini [55] observed an increase of 5.7%–9.6% in the hardness of AISI H13 steel after cryogenic treatment. In another study where traditional heat treatment and cryogenic treatment were applied to the EN 31 steel, the hardness of the cryogenically treated material was found to increase by 14% [55]. Das [52] applied conventional heat treatment and shallow and deep cryogenic processing to AISI D2 cold work tool steel. The micro hardness in the sample subjected to deep cryogenic treatment was 11.4% higher than that of the conventionally treated sample. In these studies in the literature, the increase in hardness after cryogenic processing is related to the transformation of of austenite, which is the soft phase of the material structure, to the hard martensite phase.

4. Prediction of surface roughness with ANN

In this study, a computer program was enhanced in a MATLAB platform to predict the surface roughness. The cutting tool, workpiece, cutting speed, depth of cut, and feed rate were used in the input layer of the ANN, while the surface roughness was used in the output layer. In order to obtain accurate results, a single hidden layer with 14 neurons was used. Table 4 shows the statistical evaluation of the results of the ANN with 14 neurons.

Table 5 – Weight values for surface roughness between the input and hidden layers.

$E_i = w_1x(ct) + w_2x(wp) + w_3x(V) + w_4x(dp) + w_5x(f) + \theta i$

i	w_1	w_2	w_3	w_4	w_5	θ_i
1	3.3636	−0.1659	−0.5580	2.4966	2.4454	−46.603
2	−0.5866	2.2173	0.6470	3.0316	1.3666	43.013
3	−2.7152	2.2793	−2.8487	0.6167	1.9341	37.166
4	1.5334	2.5499	−0.0755	2.6093	2.6764	−28.913
5	0.3424	−0.7709	1.1128	−2.3190	−0.8116	0.1756
6	−2.4733	−1.3852	2.3752	−2.4043	−2.7277	31.657
7	−1.9033	−2.3130	−3.2594	−1.1095	−1.1591	23.549
8	2.4317	3.5886	−0.9547	−1.3038	−2.0127	10.696
9	−0.5128	2.4649	2.2798	−2.5821	0.1085	0.9121
10	−0.2231	0.5231	−1.5641	2.1990	3.0049	−30.862
11	0.7752	1.1580	0.3817	3.1105	−4.4366	14.286
12	0.4046	−1.6768	−2.1088	2.9420	−1.8323	16.425
13	1.2932	1.9272	5.0000	0.5508	−0.5027	−41.643
14	−3.5660	−0.2142	1.9452	−1.8498	0.2100	−48.997

The matching of the experimental and ANN values for the training and the testing sets of the surface roughness are demonstrated in Figs. 10 and 11, respectively. The most dramatic point here is that the estimation values are close to the experimental values, demonstrating the estimative ability of the network for surface roughness to be satisfactory. Accordingly, the five input parameters selected as affecting factors for prediction of surface roughness provided acceptable results.

The prediction performance for both the testing and training sets of the surface roughness shows that the accuracy of the LM learning algorithm was satisfactory (± 5 %). With the ANN model developed for the prediction of the surface roughness, the RMSE values were calculated as 0.0783 and 0.0692 for training and testing data, respectively. The R^2 values for surface roughness were found to be 0.9704 and 0.9755 for training and testing data, respectively. The surface roughness can be accurately calculated by the formula given in Eq. (5).

$$\text{Surface roughness} = \left(\frac{1}{1+e^{-(-0.9334xF1+1.3933xF2-0.9928xF3+0.0687xF4-2.6078xF5-1.2896xF6-0.2625xF7-0.8741xF8-1.2553xF9+1.0164xF10-0.0424xF11+1.4785xF12+0.8252xF13+0.2526xF14+0.7824)}}\right) \quad (5)$$

where Fi (i=1, 2, …., 14) can be calculated according to Eq. (6).

$$Fi = \left(\frac{1}{1+e^{-Ei}}\right), \quad (6)$$

Ei is calculated via the equation in Table 5. The weight values for the input and hidden layers are also given in Table 5.

5. Conclusions

This study investigated the effects of cutting parameters on the surface roughness and tool wear of AISI D2 cold work tool steel with different heat treatments under dry cutting conditions using uncoated (AB30) and coated (AB2010) ceramic cutting tools. The DCTT-36 and DCT-36 treatments applied to

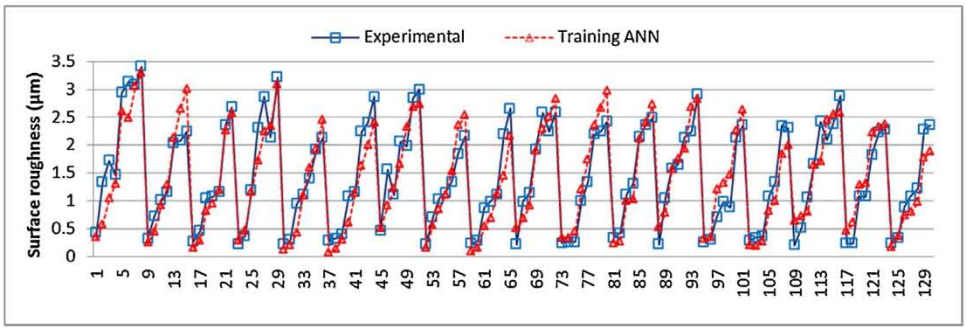

Fig. 10 – Matching of the experimental and ANN values for surface roughness training sets.

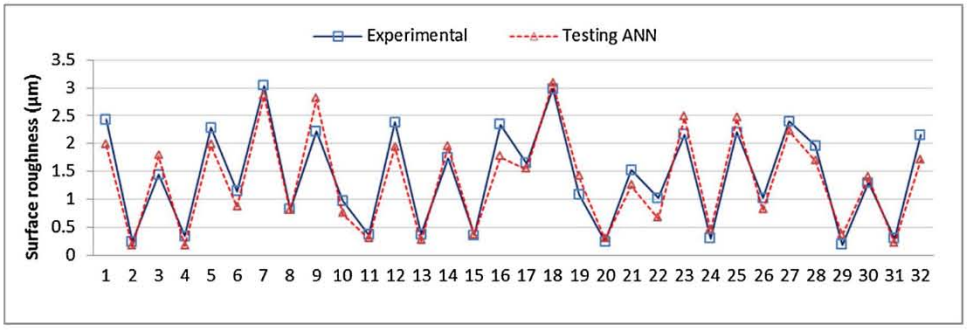

Fig. 11 – Matching of the experimental and ANN values for surface roughness testing sets.

cold work tool steel were evaluated. Finally, an ANN model was used for the prediction of the surface roughness. The back-propagation algorithm was used for training the ANN developed for determining of surface roughness. Different algorithms including BFGS, CGP, LM, RP and SCG were used for the training period. The data obtained as a result of the experimental and analytical studies conducted are given below.

- In hard turning experiments, the AB2010 coated ceramic cutting tool performed better than the AB30 uncoated ceramic cutting tool in terms of surface roughness.
- The lowest Ra value for the uncoated ceramic tool was found to be 0.2267 μm for the DCTT-36 sample at a cutting speed of 100 m/min, a feed rate of 0.08 mm/rev and a cutting depth of 0.25 mm.
- The lowest Ra value for the coated ceramic tool was found to be 0.18 μm for the DCTT-36 sample at a cutting speed of 100 m/min, a feed rate of 0.08 mm/rev and a cutting depth of 0.25 mm.
- When the workpieces subjected to different heat treatments were evaluated in the turning experiments, better Ra values were generally obtained with the DCTT-36 sample. Taking all cutting parameters and cutting tools into consideration, the DCT-36 and DCTT-36 specimens provided better surface roughness, averaging 7.56% and 10%, respectively, than the conventionally heat-treated CHT sample.
- The performance of the AB2010 coated ceramic tool was better in all of the tool wear experiments.
- At the end of the total processing time (10 min), the nose wear of the AB30 uncoated ceramic tool was measured as 0.285 mm, 0.312 mm and 0.2045 mm for the CHT, DCT-36 and DCTT-36 samples, respectively.
- Similarly, the nose wear of the AB2010 coated ceramic tool at the end of the 10-min treatment period was found to be 0.132 mm, 0.116 mm and 0.1195 mm for the CHT, DCT-36 and DCTT-36 samples, respectively. As can be seen from the nose wear results, under all cutting conditions, the lowest wear values were obtained with the DCTT-36 sample.
- When the average wear values of all the samples were measured at the end of the total machining time, the AB2010 tool exhibited better wear performance, with 54% less wear than the AB30 ceramic tool.
- Taking all the cutting parameters and cutting tools into consideration, the DCT-36 and DCTT-36 samples exhibited better nose wear at an average rate of 5.90% and 21.79% than the conventionally heat-treated CHT sample.
- At the end of the total processing time (10 min), the crater wear values of the AB30 uncoated ceramic tool were measured as 0.0684 mm^2, 0.054 mm^2 and 0.0432 mm^2 for the CHT, DCT-36 and DCTT-36 samples, respectively.
- Similarly, at the end of the 10-min processing period, the crater wear values of the AB2010 coated ceramic tool were found to be 0.0379 mm^2, 0.0332 mm^2 and 0.0298 mm^2 for the CHT, DCT-36 and DCTT-36 samples, respectively. As can be seen from the the crater wear results, under all cutting conditions, the lowest wear values were obtained with the DCTT-36 sample.
- When the averages of the crater wear values for all samples were taken at the end of the total machining time, the AB2010 tool exhibited a better wear performance of 1.4% less than the AB30 tool.

- Taking all cutting parameters and cutting tools into consideration, the DCT-36 and DCTT-36 samples exhibited better crater wear of on average 121% and 145% less than the conventionally heat-treated CHT sample.
- The best mechanical properties among the CHT, DCT-36 and DCTT-36 specimens were demonstrated by the DCT-36 sample. In the micro hardness and macro hardness measurements, the hardness values of the DCT-36 samples were higher than those of the other heat-treated samples.
- Among the three different heat treated samples, the highest hardness value was obtained with the DCT-36 sample. These results can be attributed to the deep cryogenic processing which converted the austenite phase, which has a soft structure, to the hard martensite phase in the microstructure of the material.
- As a result, the deep cryogenic and post-tempering treatments led to improvement of 32.97% in surface roughness, 21.79% in tool wear, 0.96% in macro hardness and 21% in micro hardness. The AB2010 coated ceramic tool, which generally produced better results than the uncoated ceramic inserts, led to improved surface roughness and nose wear by 25.20% and 42.21%, respectively.
- The optimal results in the prediction of the surface roughness were obtained by a network architecture of 5-14-1 and the LM learning algorithm.
- The ANN prediction performances were compared with the experimental results using R^2 and RMSE values. The R^2 values were more than 0.97 for both the testing and the training data. The RMSE value was less than 0.07 for the testing data. These results showed that the learning capacity of the ANN was relatively powerful in the estimation of the surface roughness.

Conflict of interest

The authors declare no conflicts of interest.

Acknowledgment

The authors would like to thank Düzce University Scientific Research Projects Coordinator for supporting this study with BAP project 2015.07.04.388.

REFERENCES

[1] Kara F, Çiçek A, Demir H. Multiple regression and ANN models for surface quality of cryogenically-treated AISI 52100 bearing steel. J Balk Tribol Assoc 2013;19(4):570–84, http://dx.doi.org/10.1007/s00521-014-1721-y.
[2] T. Kivak, Investigation of the influence of cryogenic process on cutting tool's drillability of Ti-6al-4v alloy, PhD Thesis, Department of Mechanical Education, Gazi University, Ankara, Turkey, 2012.
[3] Das D, Dutta AK, Ray KK. Influence of varied cryotreatment on the wear behavior of AISI D2 steel. Wear 2009;266:297–309, http://dx.doi.org/10.1016/j.wear.2008.07.001.
[4] Amini K, Akhbarizadeh A, Javadpour S. Investigating the effect of holding duration on the microstructure of 1.2080 tool steel during the deep cryogenic heat treatment. Mater Des 2012;86:1534–40, http://dx.doi.org/10.1016/j.vacuum.2012.02.013.
[5] Vahdat SE, Nategh S, Mırdamadı S. Microstructure and tensile properties of 45WCrV7 tool steel after deep cryogenic treatment. Mater Sci Eng A 2013;585:444–54, http://dx.doi.org/10.1016/j.msea.2013.07.057.
[6] F. Kara, Investigation of the effects of cryogenic process parameters on fatigue life and grindability of AISI 52100 steel, PhD Thesis, Department of Mechanical Education, Karabük University, Karabük, Türkiye, 2014.
[7] Das D, Dutta AK, Ray KK. Optimization of the duration of cryogenic processing to maximize wear resistance of AISI D2 steel. Cryogenics 2009;49:176–84, http://dx.doi.org/10.1016/j.cryogenics.2009.01.002.
[8] Amini K, Nategh S, Shafyei A. Influence of different cryotreatments on tribological behavior of 80CrMo12 5 cold work tool steel. Mater Des 2010;31:4666–75, http://dx.doi.org/10.1016/j.matdes.2010.05.028.
[9] Ozel T, Karpat Y, Figueira L, Davim JP. Modelling of surface finish and tool flank wear in turning of AISI D2 steel with ceramic wiper inserts. J Mater Process Technol 2007;189:192–8, http://dx.doi.org/10.1016/j.jmatprotec.2007.01.021.
[10] Davim JP, Figueira L. Machinability evaluation in hard turning of cold work tool steel (D2) with ceramic tools using statistical techniques. Mater Des 2007;28:1186–91, http://dx.doi.org/10.1016/j.matdes.2006.01.011.
[11] Ozel T, Karpat Y. Predictive modeling of surface roughness and tool wear in hard turning using regression and neural Networks. Int J Adv Manuf Technol 2005;4:467–79, http://dx.doi.org/10.1016/j.ijmachtools.2004.09.007.
[12] Quiza R, Figueira L, Davim JP. Comparing statistical models and artificial networks on predicting the tool wear in hard machining D2 AISI steel. Int J Adv Manuf Technol 2008;37:641–8, http://dx.doi.org/10.1007/s00170-007-0999-7.
[13] Kumar R, Sahoo AK, Das RK, Panda A, Mishra PC. Modelling of flank wear, surface roughness and cutting temperature in sustainable hard turning of AISI D2 Steel. Procedia Manuf 2018;20:406–13, http://dx.doi.org/10.1016/j.promfg.2018.02.059.
[14] Kara F. Taguchi optimization of surface roughness and flank wear during the turning of DIN 1.2344 tool steel. Mater Test 2017;59(10):903–8, http://dx.doi.org/10.3139/120.111085.
[15] Haykin S. Neural network a comprehensive foundation. New Jersey: Prentice Hall; 1999.
[16] Kara F, Aslantaş K, Çiçek A. Prediction of cutting temperature in orthogonal machining of AISI 316L using artificial neural network. Appl Soft Comput 2016;38:64–74, http://dx.doi.org/10.1016/j.asoc.2015.09.034.
[17] Arnaiz-Gonzalez A, Fernandez-Valdivielso A, Bustillo A, de Lacalle LNL. Using artificial neural networks for the prediction of dimensional error on inclined surfaces manufactured by ball-end milling. Int J Adv Manuf Technol 2016;83(5-8):847–59, http://dx.doi.org/10.1007/s00170-015-7543-y.
[18] Çay Y, Çiçek A, Kara F. Prediction of engine performance for an alternative fuel using artificial neural network. Appl Therm Eng 2012;37:217–25, http://dx.doi.org/10.1016/j.applthermaleng.2011.11.019.
[19] Özgören YÖ, Çetinkaya S, Sarıdemir S. Artificial neural network based modeling of performance of a beta-type Stirling engine. P I Mech Eng E-J Pro 2012;227(3):166–77, http://dx.doi.org/10.1177/0954408912455763.
[20] Çiftci İ. Machining of austenitic stainless steels using CVD multilayer coated cemented carbide tools. Tribol Int 2006;39:565–9, http://dx.doi.org/10.1016/j.triboint.2005.05.005.

[21] Escalona PM, Cassier Z. Influence of the critical cutting speed on the surface finish of turned steel. Wear 1998;218:103–9, http://dx.doi.org/10.1016/S0043-1648(98)00156-2.
[22] Thamizhmanii S, Kamarudin K, Rahim EA, Saparudin A, Hassan S. Tool wear and surface roughness in turning AISI 8620 using coated ceramic tool. In: Proceedings of the World Congress on Engineering. 2007.
[23] H. Gürbüz, Investigation of cutting tool geometry and coating types on surface integrity of AISI 316l steel, PhD Thesis, Department of Mechanical Education, Gazi University, Ankara, Türkiye, 2012.
[24] Fernández Landeta J, Fernández Valdivielso A, López de Lacalle LN, Girot F, Pérez Pérez JM. Wear of form taps in threading of steel cold forged parts. J Manuf Sci Eng 2015;137(3):1–11, http://dx.doi.org/10.1115/1.4029652.
[25] Gandarias A, López de Lacalle LN, Aizpitarte X, Lamikiz A. Study of the performance of the turning and drilling of austenitic stainless steels using two coolant techniques. Int J Mach Mach Mater 2008;3(1/2):1–17, http://dx.doi.org/10.1504/IJMMM.2008.017621.
[26] Kaçal A. Investigation of cutting performance of the ceramic inserts in terms of the surface roughness and tool wear at turning of PMD 23 steel. Appl Mech Mater 2014;686:10–6, http://dx.doi.org/10.4028/www.scientific.net/AMM.686.10.
[27] Özbek NA, Çiçek A, Gülesin M, Özbek O. Evaluation of the machinability of AISI 304 and AISI 316 austenitic stainless steels. J Polytech 2017;20(1):43–9, http://dx.doi.org/10.31202/ecjse.67151.
[28] Çaydaş U, Kuncan O, Çelik M. Investigation of the machinability of AISI 52100 bearing steel for surface roughness, tool life and temperature criterions. J Polytech 2017;20(2):409–17, http://dx.doi.org/10.2339/2017.20.2.
[29] Tang L, Gao C, Huang J, Shen H, Lin X. Experimental investigation of surface integrity in finish dry hard turning of hardened tool steel at different hardness levels. Int J Adv Manuf Technol 2015;77:1655–69, http://dx.doi.org/10.1007/s00170-014-6484-1.
[30] Karabatak M, Kara F. Experimental optimization of surface roughness in hard turning of AISI D2 cold work tool steel. J Polytech 2016;19(3):349–55, http://dx.doi.org/10.2339/2016.19.3.
[31] Rech J, Kusıak AJ, Battaglıa L. Tribological and thermal functions of cutting tool coatings. Surf Coat Tech 2004;186(3):364–71, http://dx.doi.org/10.1016/j.surfcoat.2003.11.027.
[32] Salımıasl A, Rafighı M. Estimation and estimation of vibration and shear force based tool wear with fuzzy logic. J Polytech 2017;20(1):111–20, http://dx.doi.org/10.2339/2017.20.1.
[33] Özbek NA. Investigation of the effects of cryogenic machining with cutting insert on tool life in processing of AISI 316 austenitic stainless steels, PhD Thesis. Ankara, Türkiye: Department of Mechanical Education, Gazi University; 2013.
[34] Lima JG, Avilla RF, Abroa AM, Faustino M, Dawim JP. Hard turning: AISI 4340 high strength low alloy steel and AISI D2 cold work tool steel. J Mater Process Technol 2005;169:388–95, http://dx.doi.org/10.1016/j.jmatprotec.2005.04.082.
[35] Jeong YK, Kang MC, Kwon SH, Kim KH, Kim HG, Kim JS. Tool life of nanocomposite Ti–Al–Si–N coated end-mill by hybrid coating system in high speed machining of hardened AISI D2 steel. Curr Appl Phys 2009;9:141–4, http://dx.doi.org/10.1016/j.cap.2008.08.053.
[36] Arsecularatne JA, Zhang LG, Montross C, Mathew P. On machining of hardened AISI D2 steel with PCBN tools. J Mater Process Technol 2006;171:244–52, http://dx.doi.org/10.1016/j.jmatprotec.2005.06.079.
[37] Poulachona G, Bandyopadhyayb BP, Jawahirc IS, Pheulpina S, Seguina E. Wear behavior of CBN tools while turning various hardened steels. Wear 2004;256:302–10, http://dx.doi.org/10.1016/S0043-1648(03)00414-9.
[38] Dosbaeva GK, El Hakimb MA, Shalaby MA, Krzanowski JE, Veldhuis SC. Cutting temperature effect on PCBN and CVD coated carbide tools in hard turning of D2 tool steel. Int J Refract Metals Hard Mater 2015;50:1–8, http://dx.doi.org/10.1016/j.ijrmhm.2014.11.001.
[39] Mavi A. The effect of cryogenic process on the cutting tool performance at the machining of Ti6al4v titanium alloy, PhD Thesis. Ankara, Türkiye: Department of Mechanical Education, Gazi University; 2014.
[40] Çiçek A, Kara F, Kıvak T, Ekici E. Evaluation of machinability of hardened and cryo-treated AISI H13 hot work tool steel with ceramic inserts. Int J Refract Metals Hard Mater 2013;41:461–9, http://dx.doi.org/10.1016/j.ijrmhm.2013.06.004.
[41] Özdemir U, Erten M. Failure mechanisms occurring in the cutting tool and tool damage the machined during abatement. J Aeronaut Space Technol 2003;1:37–50.
[42] Das D, Dutta AK, Toppo V, Ray KK. The Effect of cryogenic treatment on the carbide precipitation and tribological behavior of D2 steel. Mater Manuf Process 2007;22:474–80, http://dx.doi.org/10.1080/10426910701235934.
[43] Baldissera P, Delprete C. Deep cryogenic treatment: a bibliographic review. Open Mech Eng J 2008;2:1–11, http://dx.doi.org/10.2174/1874155X00802010001.
[44] Akhbarızadeh A, Javadpour S, Amini K. Investigating the effect of electric current flow on the wear behavior of 1.2080 tool steel during the deep cryogenic heat treatment. Mater Des 2013;45:103–9, http://dx.doi.org/10.1016/j.matdes.2012.08.012.
[45] Precıado M, Bravo PM, Alegre JM. Effect of low temperature tempering prior cryogenic treatment on carburized steels. J Mater Process Technol 2006;176:41–4, http://dx.doi.org/10.1016/j.jmatprotec.2006.01.011.
[46] Yi J, Xue W, Xie J, Liu ZP, Cheng W, Chen LX, et al. Enhanced toughness and hardness at cryogenic temperatures of silicon carbide sintered by SPS. Mater Sci Eng A 2013;569:13–7, http://dx.doi.org/10.1016/j.msea.2013.01.053.
[47] Sonawane SA, Tripathi VK, Ambekar SD. Wear behavior of cryogenic treated M2 tool steel under dry sliding condition. Appl Mech Mater 2015;798:395–401, http://dx.doi.org/10.4028/www.scientific.net/AMM.798.395.
[48] Nanesa HG. Influence of cryogenic treatment on microstructure and mechanical properties of high strength AISI D2 tool steel, Ph.D. Thesis. Canada: Université Du Québec; 2016.
[49] Das D, Dutta AK, Ray KK. Sub-zero treatments of AISI D2 steel: part II. wear behavior. Mater Sci Eng A 2010;527:2194–206, http://dx.doi.org/10.1016/j.msea.2009.10.071.
[50] Das D, Ray KK. Structure–property correlation of sub-zero treated AISI D2 steel. Mater Sci Eng A 2012;541:45–60, http://dx.doi.org/10.1016/j.msea.2012.01.130.
[51] Çiçek A, Kara F, Kıvak T, Ekici E, Uygur I. Effects of deep cryogenic treatment on the wear resistance and mechanical properties of AISI H13 hot-work tool steel. J Mater Eng Perform 2015;24(11):4431–9, http://dx.doi.org/10.1007/s11665-015-1712-x.
[52] Das D, Dutta AK, Ray KK. Sub-zero treatments of AISI D2 steel: part I. Microstructure and hardness. Mat Sci Eng 2010;527:2182–93, http://dx.doi.org/10.1016/j.msea.2009.10.070.
[53] Oppenkowski A, Weber S, Theisen W. Evaluation of factors influencing deep cryogenic treatment that affect the properties of tool steels. J Mater Process Technol

2010;210:1949–55, http://dx.doi.org/10.1016/j.jmatprotec.2010.07.007.
[54] Amini K, Negahbani M, Ghayour H. The effect of deep cryogenic treatment on hardness and wear behavior of the H13 tool steel. Metall Ital 2015;107(3):53–8, http://dx.doi.org/10.1080/10426910701235934.
[55] Harish S, Bensely A, Lal M, Rajadurai DA, Lenkey GB. Microstructural study of cryogenically treated en 31 bearing steel. J Mater Process Technol 2009;209:3351–7, http://dx.doi.org/10.1016/j.jmatprotec.2008.07.046.